Published in final edited form as:

ACS Infect Dis. 2020 February 14; 6(2): 291–301. doi:10.1021/acsinfecdis.9b00355.

Comparative structural study of terminal ends of lipoarabinomannan from mice infected lung tissues and urine of TB positive patient

Prithwiraj De[1,¶], **Libin Shi**[1,¶], **Claudia Boot**[2], **Diane Ordway**[1], **Michael McNeil**[1], **Delphi Chatterjee**[1,*]

[1]Mycobacteria Research Laboratories, Department of Microbiology, Immunology and Pathology, Colorado State University, 1682 Campus Delivery, Fort Collins, CO 80523, USA

[2]Central Instrument Facility, Department of Chemistry, Colorado State University, Fort Collins, CO 80523, USA

Abstract

Mycobacterium tuberculosis lipoarabinomannan (LAM) is a biomarker for active TB disease. The presence of LAM in urine of TB patients, whether HIV positive or negative has been validated by a gas chromatography/mass spectral method with good specificity (84%) and sensitivity (99%). However, point-of-care (POC) methods to detect TB LAM in urine using immunoassays have poor sensitivity and are limited to only HIV co-infected TB diagnosis. We hypothesized that these disappointing results with the POC methods may be due to the antibodies used in the immunoassays as there could be structural differences between LAM *in vivo* vs. LAM *in vitro*. To address this issue, we infected C3HeB/FeJ mice with *M.tb W. Beijing* SA161, and purified LAM from the lung. Analysis of these sources of LAM using a panel of existing mAbs revealed differences in epitope patterns. Conventionally, the non-reducing termini of LAM are identified by their release with endoarabinanase. These epitopes correspond to linear tetra-(Ara_4), a branched hexa-(Ara_6) arabinofuranosides and their mannose-capped versions. We discovered two distinct epitopes. In the first case it was found that the non-reducing termini of LAM from *M.tb* strain SA161 are highly succinylated, especially when the LAM was isolated from the mouse lungs. In the second case it was found that *Cellulomonas* endoarabinanase digestion of LAM from both SA161 and LAM from a TB+ HIV- patient's urine yielded epitopes based on 5 arabinoses as major components and a profound lack of Ara_6. The epitopes based on 5 arabinoses from *M.tb* SA161and from the LAM in human urine must result from underlying structural and thus epitope differences. These results suggest approaches to develop specific antibodies for POC tests for LAM in urine of suspected TB patients.

Keywords

urinaryLAM; Mlung-LAM; Cul-LAM; LAM epitopes; LAM structure; LC/MS-MS; C3HeB/FeJ mice

* Corresponding author: Delphi.chatterjee@colostate.edu, Phone 970 491 7495.
¶These authors contributed equally to this work

Mycobacterium tuberculosis (*M.tb*) is a major cause of death worldwide. Globally, an estimated 10.0 million people fell ill with TB in 2018. The burden of disease varies enormously among countries, from fewer than five to more than 500 new cases per 100 000 population per year. There were an estimated 1.2 million TB deaths among HIV-negative people in 2018, and an additional 251 000 deaths (range, 223 000–281 000) among HIV-positive people [1].

It has been stated that between years 2000–2015, 49 million lives were saved through effective diagnosis and treatment, yet TB remained one of the top ten causes of death worldwide in 2015 [2]. Yet, despite the emergence of multiple and extensively drug resistant strains (MDR/XDR), TB is largely a curable disease. Why then do so many people still die from TB? A primary reason is that the methods used for diagnosing the disease are inadequate. Indeed, over 1.5 million people in India alone undergo useless TB tests each year and 40% of all active TB cases in the world are estimated to remain undiagnosed (50% in Africa) [3].

LAM is a cell wall lipoglycan specific to the mycobacterium species. It is associated with the bacterial cell surface as well as anchored in the plasma membrane[4–6]. Structurally, LAM from the *in vitro* grown mycobacterium (Cul-LAM) is complex and highly heterogeneous. It is characterized by three distinct structural domains (Fig. 1): (i) a phosphatidylinositol anchor, (ii) a mannan backbone, and (iii) several arabinan antennas emanating from the mannan backbone. The terminal Ara_4 (β-D-Ara*f*-(1→2)-α-D-Ara*f*-(1→5)-α-D-Ara*f*-(1→5)- α-D-Ara*f*) tetrasaccharide and Ara_6 ([β-D-Ara*f*-(1→2)-α-D-Ara*f*-(1-)$_2$ →3, and→5]-α-$_D$-Ara*f*-(1→ 5)-α-D-Ara*f*) hexasaccharide have been shown to be the dominant epitopes recognized by anti-LAM monoclonal antibodies (mAb) [6–11], such as the CS-35 mAb illustrated in Fig 1. In the pathogenic mycobacterial species (e.g. *M.tb*, *M. leprae*, *M. avium*), the termini of the arabinan are further tethered with short mannan caps (di- or tri-saccharide)[12, 13], resulting in the mannosylated LAM (ManLAM).

It has been postulated that LAM is released from metabolically active or degrading mycobacterial organisms into the serum, with subsequent filtration by the kidneys, passing into the urine where it can be detected by an enzyme-linked immunosorbent assay (ELISA). LAM is a highly immunogenic molecule frequently associated with anti-LAM antibodies readily detectable in serum [14]. Systemically released LAM may circulate in large immune complexes [15], which would not be able to pass through normal renal glomeruli to the urine [16]. In another possibility, free or antibody-complexed LAM released from mycobacteria within the renal tract could pass directly into urine without the need to pass through the glomerular membrane [17].

Till date, all of the purified LAM being used for assay development and characterization of anti-LAM antibodies is derived from bacteria cultured *in vitro*. One important question is whether LAM circulating in fluids of infected TB patients (so-called "*in vivo*" LAM) differs from the molecule produced in bacterial cultures (Cul-LAM). One possibility is that host enzymes either partially degrade the complex glycoform of LAM or modulate the structure of the sugars present at the caps that are characteristic of pathogenic strains of mycobacteria, including Mtb. We have in fact seen considerable heterogeneity in the capping structure of

ManLAM produced by *in vitro* culture [18–20]. This raises the questions of, a) which of these structures are most prevalent in patient blood and urine samples, and b) which epitopes would be the valid targets for antibody-based detection assays [21]. Recently discovered substituents such as succinyl group at the C-2 of and internal 3,5-di-α-D-Ara*f* residue and 5-deoxy-5-methylthio-xylofuranose (MTX), which attaches to one of the capping oligomannosyl chains may play a role in the immune response arising from Mtb infection [22–24]. We set out to address these issues in our present work starting with animal infection.

The low yields of viable bacilli and severe host tissue contamination reported in our earlier work prompted us to choose a clinical isolate for infection in Kramnik mice and develop a new facile and reproducible method for isolating LAM [25]. The SA161 strain was used due to the increasing evidence that clinical isolates that belong to the W-Beijing genotype of newly emerging strains are often of very high virulence when tested in small animal models, including the mouse and guinea pig [26].

In this study, we established a method for extraction and purification of lipoglycans (summarised isolation protocol in Supplementary Fig. S1) from tissues of animal models infected with *M.tb* W. Beijing clinical strain SA 161 using hydrophobic interaction chromatography (HIC) and in tandem used a similar procedure to isolate and characterize LAM from urine (U-LAM) of non HIV patients with active TB. Although rigorous purification was not possible due to paucity of LAM in the tissues and urine with heavy contamination with host glycans, we developed sensitive analytical tools and were able to easily characterize the non reducing ends of LAM “in vivo”using sensitive LC/MS-MS from our correct undertanding of the LAM “ in vitro” structure.

Results

Preparation and Purification of *in vitro* (culture grown) LAM (Cul-LAM) from *M.tb* SA161

Bacilli were grown on 7H11 OADC plates at 37^0C for over three weeks, collected, washed and LAM was isolated from pelleted bacilli using procedure as described below omitting the homogenization and enzyme treatment steps.

Preparation and purification of LAM from mice infected with *M. tb* W. Beijing SA161

In the Kramnik mouse model (C3HeB/FeJ), the *M.tb* load increases to high numbers and the lung pathology progresses dramatically following a low-dose infection. Kramnik mouse lung tissues can develop highly organized encapsulated necrotic lesions that mimic those of human TB patients.

W. Beijing SA161 was adapted to infect mice. Out of 30 mice, 20 were used for infection, while the other 10 were treated as negative control. In order to further improve the bacterial load in the infected lung tissues, the mice were infected with a high dose of *M.tb* SA161 (1×10^7/mL) via aerosol. At day 30, all the animals were sacrificed, lungs from 4 animals were used for CFU counts, and lungs from the other 16 infected animals (Fig. 2) and 10 naïve controls were stored. As shown in Fig. 2, the bacterial load was more than 10^{10} per SA161 infected lung, which was 3–4 logs higher than that of low dose aerosol infected guinea pig lung tissues.

Isolation and Purification of LAM

Due to the evidence showing that C3HeB/FeJ mouse lung tissues can develop highly organized encapsulated necrotic lesions that mimic those of human TB patients [27] and to improve the yield of LAM *in vivo* and characterize, we homed in on SA161 infected C3HeB/FeJ mouse lung tissues for extraction and purification (Supplementary Fig. S2)

In order to extract LAM Kramnik mouse lungs were homogenized and subjected to enzyme digestion. After centrifugation, the pellets were delipidated and disrupted by sonication. The suspension was extracted with aqueous phenol, the aqueous layer was dialyzed and used for downstream analyses. Similar extraction method was also used for uninfected mouse lungs as negative control and for the bacilli grown on 7H11 OADC plates at 37°C for 3 weeks as positive control.

The LAM preparation at this stage after probing with SDS-PAGE followed by Periodic acid–Schiff (PAS)-silver staining and western blot using Concanavalin A showed contamination with host glycans (data not shown). In addition, the glycans extracted from naïve tissues showed some non-specific reactions with the anti-LAM mAbs. Therefore, lipoglycans isolated from infected tissues, negative controls and in vitro grown bacilli were all subjected to the HIC column with Octyl Sepharose [28].

The column was eluted with a stepwise gradient buffer of 0.1 M ammonium acetate containing 5%, 15%, 40% and 65% n-propanol. These four fractions were collected and dried under nitrogen. For each fraction, monosaccharide composition analysis by GC/MS and reactions to pooled mAbs by western blot analysis were performed. LAM typically eluted at 40% propanol fraction devoid of majority of contaminating neutral glycans, and was used for subsequent analysis [23].

Quantification of Cul-LAM and Mlung-LAM by Gas Chromatography-Mass Spectrometry (GC/MS)

For sugar composition analysis, a neutral sugar standard with known amounts of monosaccharides (rhamnose, arabinose, ribose, fucose, mannose, galactose and glucose) and an aliquot of HIC purified LAM samples was processed using 3-*O*-methylglucose as the internal standard. The samples were hydrolyzed, reduced and then converted to alditol acetates and analyzed by GC/MS. As shown in the supplementary Fig. S3, there was no detectable arabinose in the putative lipoglycans extracted from naïve C3HeB/FeJ mouse lung tissues; presence of trace amount of mannose could be from the host glycan contamination. For the Mlung-LAM and Cul-LAM preparations, both arabinose and mannose were detected. Since mannose may also originate from host in the in vivo preparation rather than LAM/LM, the amount of LAM in each sample preparation was calculated based on the amount of arabinose measured. As the amount of arabinose accounts for about 60% of LAM composition, the yield of LAM was estimated to be about 6 ~7 ug LAM per infected lung.

Western Blot analysis on Mlung-LAM

The Mlung-LAM, Cul-LAM and negative control samples were first analyzed by SDS-PAGE followed by Western Blot analysis with pooled mAbs. As shown in Fig. 3 A, there was no reaction to the lipoglycans from uninfected lung tissues. In comparison to the Cul-LAM the spread of Mlung-LAM was lesser suggesting it may be more homogenous.

In order to examine if there is any difference in affinity of the two LAM preparations to individual antibodies, 50 ng of LAM samples (based on GC-MS Arabinose quantification) were analyzed by SDS-PAGE followed by WB analysis. As shown in Fig. 3B, Mlung-LAM had a very strong reaction to mAb CS40, however, Cul-LAM had negligible reaction. Both LAM samples showed strong reactions to CS35 and ML34, but weak reactions to 922.5, 906.7 and 908.1. To mAbs of 906.45 and 906.8, neither of the LAM showed any reaction. Out of these mAbs, the motifs recognized by mAb CS35 and the 900 series (generated against *M. leprae*) [29] are the terminal branched Ara_6 and linear Ara_4 whereas CS40 (generated against LAM from the virulent Erdman strain) are to the mannose capped Ara_6 [13].

Analysis of nonreducing ends of LAM-arabinan by LC/MS

We have shown that LAM-arabinan can be digested using enzymes secreted by species of *Cellulomonas gelida* that was isolated from soil by culture enrichment [30, 31]. The enzyme releases non-reducing termini whether or not they are mannose capped. The endoarabinanase also released some internal disaccharide, Ara_2 α-D-Ara*f*-(1→5)-D-Ara*f* in an unknown fashion. In this study, Cul-LAM and Mlung-LAM preparations were digested with endoarabinanase, and completion of digestion was ensured by SDS/PAGE (Fig. 4 A, B). For the Mlung-LAM, a stained smear was observed extending from the loading well to about 35kDa, which could arise from host glycan that is resistant to the endoarabinanase [23, 30]. The enzyme digested preparation was subjected to a Centricon membrane separation (3kDa MWCO) to broadly separate the enzyme resistant mannan core and obtain the oligoarabinosides in the flow through. LC/MS showed that oligoarabinoside profile on the non reducing end of the two LAM preparations were very similar except for the higher abundance of and $Man_{0–4}Ara_5$ and succinylation (Fig. 5).

Importantly both LAM preparations showed major ions corresponding to $Man_{0–4}Ara_5$. Ara_5 based components in major amounts has not been reported before.

All the MS data are presented in the Supplementary Table S1.

Succinylated LAM arabinan ($(Man)_{0–6}Ara_{4–6}$) termini

In our analyses, an increase in mass by 100 Da should correspond to a succinyl-residue [32]. We noticed a dramatic increase in the abundance of monosuccinylated-Ara_4 (*m/z* 645.188 $(M\text{-}H)^{1-}$; **1a**; Fig. 6); Ara_5 (*m/z* 777.230 $(M\text{-}H)^{1-}$), Man_1Ara_5-I (*m/z* 939.283 $(M\text{-}H)^{1-}$; **2a**; Fig. 7), Man_2Ara_5-I (*m/z* 1101.336 $(M\text{-}H)^{1-}$) and Ara_6 (*m/z* 909.272 $(M\text{-}H)^{1-}$) for Mlung-LAM compared to Cul- LAM. As a major LAM terminus, monosuccinylated Ara_4 is expected to have β-D-Ara*f*-(1→2)-α-D-Ara*f*-(1→5)-α-D-Ara*f*-(1→5)- α-D-Ara*f*-(1→5) sequence of arabinofuranose units. In order to investigate the location of succinyl-residue,

the ion at *m/z* 645 (M-H) $^{1-}$ (**1a**) was subjected to MS^2 analysis. The ion at *m/z* 599 (M-H) $^{1-}$ corresponding to a neutral loss of 46 Da (formic acid; α-cleavage) accounts for the presence of a carboxylic acid function as part of succinate (100 Da). The ion at *m/z* 545 (M-H) $^{1-}$ (**1b**) accounts for the loss of succinyl residue and a loss of 118 Da gave the ion at *m/z* 527 (M-H) $^{1-}$ (**1c**) that suggests the succinate is attached to a secondary alcohol i.e, either 2- or 3- position giving a more stable endocyclic double bond in the product ion. It is less likely that a cleavage from a primary alcohol (as in 5-position) should give a stable exocyclic olefin in the product ion [33]. The abundant ion at *m/z* 455 (M-H) $^{1-}$ ($^{0,2}X_2$; **1d**) accounts for a loss of 190 Da, as $^{0,2}A_1$ ion, suggesting that the succinyl residue is possibly attached at the non-reducing end. The presence of ion at *m/z* 143 ($^{0,2}A_1$-46; **1f**), due to α-cleavage (loss of 46 Da), supports this assignment. Further, the ion at *m/z* 455 (M-H) $^{1-}$ (**1d**) did not have a paired peak at *m/z* 437 (M-H) $^{1-}$, i.e, a further loss of 18 Da, suggesting the loss of succinyl residue was integrated to the $^{0,2}A_1$ cross ring fragmentation. Also, the ion at *m/z* 555 (M-H) $^{1-}$ ($^{0,3}A_3$) possibly arising from the sequential loss of 60 Da (*m/z* 585 (M-H) $^{1-}$; $^{0,2}A_3$;**1e**) followed by a loss of 30 Da at the reducing end, as shown in the figure, clearly indicate that the succinyl residue is not at the reducing end. It can be argued that this loss of 190 Da can also be associated to the terminal β-Ara*f*. The presence of ion at *m/z* 537 (M-H) $^{1-}$ ($^{0,3}X_{3\alpha}$; **1g**) due to the loss of 62 Da from *m/z* 599 (M-H) $^{1-}$clearly indicate that the terminal β-Ara*f* has unsubstituted 3- and 5-OH groups. However, the formation of *m/z* 113 $(M-H)^{1-}$, a furan-derivative, seems only possible when a pentose (Ara*f*) is branched i.e, it has substituents in 2- or 3-position as explained in the Fig. 5. It possibly involves a γ-elimination mechanism [34]. The attainment of aromaticity probably confers the stability to the product ion (Fig. 6). Therefore, the presence of *m/z* 213 (4-((2-(hydroxymethyl)furan-3-yl)oxy)-4-oxobutanoate; **1h**), a D type ion, clearly suggest that the succinyl residue is at the 3-hydroxyl substitution of the 2-glycosylated arabinose (the penultimate Ara*f* at the non-reducing end).

With a convincing fragmentation pattern showing the location of the succinyl residue for Ara_4, we wanted to explore the structural alignment of the relatively abundant Ara_5 termini. We chose to subject the ion *m/z* 939 $(M-H)^{-1}$(**2a**; Fig. 7), that corresponds to Man_1Ara_5Suc, to MS^2 fragmentation. A characteristic loss of 190 Da as the $^{0,2}X$-type ion at *m/z* 749 $(M-H)^{1-}$ ($^{0,2}X_3$; **2b**) was observed. A loss of succinate was observed, as before, giving ions at *m/z* 839 $(M-H)^{1-}$ (M-100) and *m/z* 821 $(M-H)^{1-}$ (M-118), confirming our earlier assignment that it is linked to a secondary alcohol (3-substitution). The presence of ions at *m/z* 569 $(M-H)^{1-}$ ($^{0,2}A_2$-46; **2c**), *m/z* 539 $(M-H)^{-1}$ ($^{0,3}A_2$-46; **2d**) and *m/z* 257 $(M-H)^{1-}$ ($Z_{4\alpha}-^{0,2}A_2$-46; **2e**) clearly shows the presence of the succinyl residue at the 3-position of 2-linked Ara*f*. However, sequential losses of 132 Da and the cross ring fragments, as explained in the Fig. 7; **2a-b**) supports a linear arrangement (i.e, β-D-Ara*f*-(1→2)-α-D-Ara*f*-(1→5)-α-D-Ara*f*-(1→5)- α-D-Ara*f*-(1→5))- α-D-Ara*f*) for Ara_5 termini. Although, the ions such as *m/z* 557 $(M-H)^{1-}$ (**2f**, **2f'**) or *m/z* 425 $(M-H)^{1-}$ (after a loss of 132 Da from **2f, 2f'**) can be found for a branched Ara_5 alignment (i.e, β-D-Ara*f*-(1→2)-α-D-Ara*f*-[α-D-Ara*f*-(1→3)]-(1→5)-α-D-Ara*f*-(1→5)- α-D-Ara*f*) as well, absence of all of the D-type ions (**2g-j**) at *m/z* 639 $(M-H)^{1-}$, *m/z* 593 $(M-H)^{1-}$ (**inset** Fig. 7), *m/z* 521 $(M-H)^{1-}$ and/or *m/z* 449 $(M-H)^{1-}$ suggested that Man_1Ara_5 or Ara_5 termini has a linear arrangement. In the supplemental section Fig S4 explains MS^2 spectrum of branched structure of Ara_5, as obtained from

Arabinogalactan (AG) that fits the loss of a single β-T-Ara from Ara_6 and is distinct from LAM (linear $Ara_{5)}$.

However, it is likely that a branched Ara_6 would give a more complex fragmentation pattern as evident from MS^2 spectrum of Man_4Ara_6-II (*m/z* 728.230 $(M\text{-}2H)^{2-}$). The detailed analysis (Supplementary Fig. S5) suggest that the Ara_6 is branched and moreover, reveals that both the arabinan arms are equally mannose-capped with α-D-Man*p*-(1→2)-α-D-Man*p*-(1→2)- units.

MTXMan_1Ara_5

MTX is a unique structural feature for mannose-capped TB LAM. It is expected to be one per molecule of LAM, making it less abundant. We identified low intensity ions that corresponded to MTXMan_1Ara_5 (*m/z* 1001.30 $(M\text{-}H)^{1-}$) overlapping with Man_2Ara_5 (*m/z* 1001.32 $(M\text{-}H)^{1-}$) in both in Cul-LAM and Mlung-LAM (Fig. 8). Such a small difference in *m/z* values coupled with low abundance made it difficult to unambiguously confirm the presence/absence of MTX. Therefore, we applied sodium borodeuteride pre-reduction followed by permethylation to the mixture of enzyme released arabinosides and analyzed the products with ES/MS in the positive mode. The permethylated MTXMan_1Ara_5 was now detected at *m/z* 1261.7 $(M+NH_4)^{1+}$ and 1266.6 $(M+Na)^{1+}$ and Man_2Ara_5 was detected at 1289.68 $(M+NH_4)^{1+}$ and 1294.6 $(M+Na)^{1+}$ (Fig. 8). The chromatogram and MS data on MTXMan_1Ara_5 from Cul-LAM has been presented in the Supplementary Fig. S6). However, paucity of sample did not allow us to confirm MTX-termini using MS^2.

C) $(Man)_{0-6}$-Ara_{7-8} and/or lactyl/acetyl LAM arabinan termini

The presence of Ara_7, Ara_8 or higher arabinan and their mannose-capped versions in LAM have been reported earlier [31]. The possible occurance of succinyl substitution directed us to assess the presence of other acyl functions such as lactate, as reported earlier [35]. Unfortunately, the *m/z*-values of Ara_7-and higher and their mannose-capped variation and $((Man)_{0-6}$-$Ara_{4-6})$ lactate or $((Man)_{0-6}$-$Ara_{4-6})$ acetate were found to be same. Both singly-charged and doubly-charged ions for these termini were noticed (Supplementary Table S2). Low abundance of these ions did not allow us to confirm the structure by MS^2 fragmentation. The pre-reduction-permethylation approach did not help because of the same *m/z* values and moreover, they remove all acyl-function linked through ester-linkage. However, earlier report mentioned that the lactyl substitution could possibly attached through ether-linkage. We saw multiple and or overlapping peaks in some extracted-ion chromatogram from ESI-LC/MS (positive) of permethylated arabinan termini corresponding to the same ion. For example, *m/z* 1609.9 $(M+NH_4)^{1+}$ from Mlung-LAM corresponds to permethylated Man_2Ara_7 as well as permethylated Man_4Ara_4Lactate and both the peaks in EIC (Fig. 9) shows the same ion. These may suggest the presence of either both lactate substitution and Ara_7 or higher termini or their structural variants. The low abundance of these ions requires larger volume of TB patient's urine sample to be processed to resolve the structural issues with certainty.

Characterization of U-LAM and its comparison with Mlung LAM after reduction and methylation

For U-LAM analysis, dialyzed TB+ve urine samples PB2 and PB4 (~40 mL each; containing LAM ~40 ng/mL and 25 ng/mL respectively, estimated from GC/MS analysis) was passed through Octyl Sepharose column purification and subsequently eluted (confirmed by spike in experiments with nitrocellulose dot blot) with the 40% and 65% propanol [28]. The LAM containing fractions was digested with endoarabinanase, and the arabinan fragments obtained as the flow-through using membrane (3 kDa MwCO) filtration. The samples were dried and PB2 was subjected to ESI-LC/MS directly. However, the profile did not give enough ions in the negative ionization mode. The oligosaccharides in the sample PB4 were reduced and per-*O*-methylated and analyzed by LC/MS (Fig. 9).

The permethylated arabinosides of PB4 was subjected to ESI-LC/MS in the positive ion mode. The reduced and methylated oligosaccharides were identified by the value of the $(M+NH_4)^{+1}$ ions and the intensity of these ions were used to calculate the relative percent of the oligosaccharides found (Fig. 9). The ions for Ara_2 (*m/z* 400.2 $(M+NH_4)^{1+}$), Ara_4 (*m/z* 720.4 $(M+NH_4)^{1+}$) and Ara_5 (*m/z* 880.4 $(M+NH_4)^{1+}$) were found but no detectable amount of Ara_6 (*m/z* 1040.5 $(M+NH_4)^{1+}$) or its mannose capped variants were detected. The bar plot (Fig. 9) shows the relative abundance of the methylated oligoarabinosides. Among Ara_4 and its mannose-capped version, non-mannosylated Ara_4 was dominant. The presence of Ara_5 with $(Man)_{0–6}$- caps were identified at *m/z* 880.4 $(Ara_5 + NH_4)^{1+}$, 1084.5 $(Man_1Ara_5+ NH_4)^{1+}$ 1288.6 $(Man_2Ara_5+ NH_4)^{1+}$, 1492.7 $(Man_3Ara_5 + NH_4)^{1+}$, 1696.8 $(Man_4Ara_5 + NH_4)^{1+}$, 1900.9 $(Man_5Ara_5 + NH_4)^{1+}$ as dominant species. Noticeably, ion corresponding to $MTXMan_1Ara_5$ at *m/z* 1260.6 $(M+NH_4)^{1+}$, as found in Cul-LAM, was also identified. (Supplementary Fig. S7)

Discussion

Although LAM has been the subject of intense research and diagnostic efforts, clinical tests of a commercial LAM ELISA assay have been highly inconsistent in terms of both sensitivity and specificity, with most studies concluding that LAM is a promising target for certain populations (particularly HIV+ patients), but it has yet to live up to its full diagnostic potential. Two commercial tests are worth mentioning here, the ALERE TB LAM test and the new (yet to be in the market) FujiLAM Test. Both tests are simple, urine LAM based Lateral Flow assays. The Alere LAM test is highly specific but lacks sensitivity ~(40%) (works only in HIV +ve patients and the FujiLAM test is reported to be more sensitive (~70%) than Alere and only targets HIV +ve patients. A primary objective remained that LAM has not yet been validated conclusively as an *M.tb* biomarker for reasons such as antibodies used lack the affinity and specificity needed to detect it in the presence of non-cognate oligosaccharides that do not present the same epitope as in urinary LAM. We thus sought to explore the structure of LAM for the first time, from infected tissues from animals and urine samples from TB patients. After several trials and optimization we focused on an improved method of isolation of Mlung-LAM from the C3HeB/FeJ mouse infection model and purified Mlung-LAM from the resulting necrotic lung. Concomitantly, we isolated LAM from a TB+ HIV- patient's urine (U-LAM). Comparative analysis of two sources of LAM

(Cul-LAM and Mlung-LAM) using a panel of existing mAbs currently used for developing LAM based diagnostic platforms revealed differences in epitope patterns suggesting differences in the terminal arabinan structure. Following this initial observation, the LAM preparations were deeply analyzed using enzyme digestion, high resolution MS followed by MS^2 analyses and showed major structural differences in the terminal end.

Previously we have shown that LAM-arabinan can be digested using endoarabinanase [31]. Major digestion products from any Cul-LAM were found to be Ara_6, and Ara_4 along with some Ara_5 and Ara_2. In this study, we anticipated the possible presence of acyl functions and therefore, developed a LC/MS approach for analyzing native oligosaccharides using negative-ion mode. Results indicate that Cul-LAM, from *M. tb* W. Beijing SA161 has a high abundance of branched Ara_6, succinylated Ara_6, and moderate abundance of their mannose-capped variations. Linear Ara_4 and Ara_5 and their mannosylated and succinylated variations were also present albeit in low abundance. On the contrary, in the Mlung-LAM, succinylated Ara_4, Ara_5 motifs were dominant (Fig. 5; Supplementary Fig. S8). The most notable finding was the presence of a succinyl residue on all the linear Ara_4, and Ara_5 motifs. MS^2 analysis clearly established that the succinyl residue is at the 3-OH of the 2-linked penultimate Ara*f*. It has been reported that succinyl residues are present in both LAM and AG from *M. tb*, H37Rv [36, 37] however, the attachment sites of succinyl residue to the Ara*f* were different from what we established here.

The MS analyses also indicated the possibility of the presence of a lactate and acetate covalently linked in the non reducing ends of LAM but the low abundance and potential overlap of some of these substituents with isomeric structures, prevented us from doing any MS^2 analyses. Incidentally, the presence of lactate groups, associated with the arabinomannan domain of LAM, was also reported in *M.tb*, *M. smegmatis* and *M. leprae*[35]. Methylthio xylose (MTX) is a unique structural feature for mannose-capped TB LAM[23, 38]. Confirmation of the presence of this residue was obtained after permethylation of prereduced mixture of oligo-arabinosides and analysis with ESI/MS in the positive mode.

For U-LAM analysis, we had to adapt a separate approach due to limited amounts of LAM available. The enzyme released oligoarabinosides could not be analyzed in their native forms but were pre-reduced and methylated and then subjected to reverse phase LC/MS. This would essentially remove all the acyl functions identified in Mlung-LAM if these were present. We obtained a very simplistic oligoarabinofuranoside profile (Fig. 9) with dominating Ara_5 and Ara_4 species both with and without mannose-capping however, most noticeable difference being the virtual lack of terminal Ara_6 motif in U-LAM which is alarming as it is a major LAM epitope that is recognized by almost all of the existing mAbs. This fact might be arising due to either of the two reasons i) the terminal Ara_6 epitopes are not present in U-LAM and there is some processing of LAM as it travels from the site of infection into the urine; ii) this particular urine sample may have altered arabinan architecture due to a strain variation. In summary, we have now seen that Cul-LAM and Mlung-LAM originating from identical strain when grown in culture vs. in a host are similar. Most importantly, when LAM passes from lung to urine, or during infection there could be further processing of LAM (such as with endogenous enzymes) which would ultimately yield a simplistic arabinan with linear Ara_5 motifs. We believe that the predominant Ara_5 in

U-LAM is β-D-Ara*f*-(1→2)-α-D-Ara*f*-(1→5)-α-D-Ara*f*-(1→5)- α-D-Ara*f*-(1→5))- α-D-Ara*f* similar to the linear Ara_4 based on the endoarabinanase specificity [30].

LAM from a *M. tb* culture (Cul-LAM) has been well-characterized for its importance in providing *M.tb* a safe entry to phagocytes, regulating the intracellular trafficking network, as well as immune responses of infected host cells [39–41]. These LAM immunological characteristics are thought to be linked to the subtle but unique and well-defined structural characteristics of this molecule, including but not limited to the degree of acylation, the length and composition of the D-mannan and D-arabinan, the length of the mannose caps, as well as the presence of other acidic constituents such as succinates, lactates and also the presence of 5-methylthioxylose [23, 24, 42]. The fact that our present work on the Cul-LAM suggests that all these substituents are present in the Mlung-LAM but perhaps on a different terminal arabinan structure is intriguing and may explain some of the varied binding response to the available mAbs.

Conclusion-LAM structure-antibody relationship

The observed differences in antibody recognition pattern between Cul-LAM and Mlung-LAM, (Fig. 3B), can be explained by the epitope selectivity. In our earlier report, we evaluated several antibodies against 12 synthetic glycoconjugates pertaining to LAM arabinan termini[9]. Among those, CS35 raised against *M. leprae*[29] was found to have a broad range affinity. The indirect ELISA response being the indicator of avidity towards a particular epitope of the antigen [43], only 3 epitopes Ara_6, Man_4Ara_6, and $MTXManAra_6$ had OD values >1 with CS35 indicating that it has a preference for branched Ara_6 termini. The presence of Man_4Ara_6 and Ara_6 as dominant arabinan termini in both Cul-LAM and Mlung-LAM accounts for their equal response on the Western Blot (Supplementary Fig. S7). However, the mAb CS40 (Mtb, Erdman LAM)[13] only detected the Mlung-LAM. This mAb had a distinct avidity (OD>2.7) towards 4 synthetic glycoconjugates; Man_1Ara_4, $Man_{1\times2}Ara_6$, $MTXMan_1Ara_4$ and $MTXMan_1Ara_6$ indicating that CS40 is specific for singly mannosylated Ara_4 and Ara_6 termini. Incidentally, Man_1Ara_4, Man_1Ara_5 and Man_1Ara_6 and their succinylated analogs are visibly more abundant in Mlung-LAM. Whether the presence of succinyl-residue at the mAb-recognition region affects the antibody response or not needs further investigation and could be very important. It is interesting to note that X-Ray crystallographic structure of CS35 with Ara_4 and Ara_6 have been elegantly shown [44]. We now propose to include the idea of modeling succinylated Ara_4/Ara_5 into the binding pocket of CS35 (and other antibodies). Nevertheless, we do believe that there are enough non-succinylated versions of Ara_4 so that the antibodies in use still have values. The mAbs of the 900-series seem to have higher, and variable avidity (OD≥1) for Ara_4 and Ara_6. Apparently, these mAbs are specific towards non-mannose-capped arabinan termini. It is conceivable that the mAbs that have higher affinity for Man_nAra_6 may give reduced response to U-LAM as there may not be any detectable Man_nAra_6 among the epitopes. Presence/absence of Ara_6 vs. Ara_5 or succinylation may depend on host, *M.tb* strain-involved in the disease and demographic region. We are actively pursuing our research to address these issues.

Limitations of our study include negligible amounts of samples for analyses and relying heavily on mass spectrometry. Because of these reasons, our U-LAM analysis remains

incomplete as we were unable to analyze oligosaccharides in their native forms precluding the presence/absence of the succinyl function. Presence of a succinate will not only change the charge on LAM but also perhaps its affinity towards antibodies. This previously unrecognized structural modification impacts host-pathogen interaction and has implications for pathological events.

Methods and Materials

Ethics Statement and Institutional Approvals

This study conforms to the Declaration of Helsinki and was approved by the CSU Institutional Biosafety Committee (IBC) and Integrity and Compliance Review Board under approval human IRB protocol number 09–006B (Lipoarabinomannan Analysis in Urine and Serum) valid till 2020–03-06 and renewed annually. To prevent contamination, all samples were processed in the sterile biosafety cabinet by trained personnel. All the buffers and reagents used were sterile. Glassware for chemical derivatization were washed and baked at 550 °F (overnight) before use. Mouse infection with *M. tb* was performed under the CSU IACUC# **Protocol ID:** 12–3229A.

C3HeB/FeJ mouse infection

For a better yield of the bacilli we used C3HeB/FeJ (Kramnik) mouse model. *M. tb* W. Beijing SA161 was administered using Glas-Col aerosol chamber exposure to *C3HeB/FeJ* mice. Out of 30 mice [45], 20 were used for infection, while the other 10 were maintained as negative control. In order to improve the bacterial load in the infected lung tissues, the mice were infected with a higher dose of M.tb SA161 (1×10^7/mL) via aerosol using the same standard operating procedure [45]. At day 30, all the animals were sacrificed, lungs from 4 animals were used for CFU counts, and lungs from the 16 infected animals and 10 naïve controls were stored frozen at −80°C for further use.

CFU counts

One hundred μL homogenate samples and seven 10-fold serial dilutions for each homogenate were plated on 7H11 OADC agar quadrant petri plates and cultivated at 37 °C for about 3 weeks for CFU counts to determine the bacterial load within the organs. The bacteria grown on 7H11 OADC agar plates for CFU counts were used as the vitro controls.

Extraction of Lipoglycans from necrotic lung tissues

Frozen tissues were thawed at room temperature (RT) and weighed, and then were rinsed with phosphate buffered saline (PBS, pH 7.2, without $CaCl_2$ or $MgCl_2$). The tissues were placed in a 40 mL straight walled homogenization tube and PBS (3mL per g tissue) was added. Homogenization was performed by using a Tissue-Tearor followed by further homogenization using a variable speed motor drive homogenizer and Teflon pestle at 4,000 rpm for 15 passes.

In order to extract LAM, homogenized tissues were subjected to collagenase (1 mg/mL) digestion at 37°C for 4 hrs followed by pronase E (0.5 mg/mL) treatment for overnight. The

mixture was centrifuged to obtain pellets, and the pellets were delipidated. The same protocol was also used to extract naïve mice lungs as negative control.

Bacterial load in C3HeB/FeJ mouse lung tissues

High dose aerosol infection with SA161 was selected to infect *C3HeB/FeJ* mouse. And the bacterial yield was more than 10^{10} per SA161 infected lung, which was 3–4 logs higher than that of low dose aerosol infected guinea pig lung tissues. (Fig. 3)

Isolation of lipoglycan from infected lung tissues

The enzyme digested homogenate was centrifuged at 10,000xg for 15 minutes at 4°C to obtain pellets containing the bacilli. The pellets were suspended in 20 mL chloroform: methanol (2:1) and rocked at RT for 2–3 days and then centrifuged at 3,000 rpm for 15 minutes. The pellets were suspended in 20 mL chloroform: methanol: water (10:10:1.5) and rocked at RT for 24 h. The delipidated mass was centrifuged at 3,000 rpm for 15 min at RT. The pellets were suspended in water and PBS-saturated phenol (1:1) and incubated at 80 °C for 3 hours with stirring. The sample was centrifuged at 3,000 rpm for 20 minutes at RT to get the separation of two layers. The extraction with water/PBS-saturated phenol was repeated two more times by adding equal volume of water to the organic (lower) layer. The combined aqueous layers were dialyzed overnight and then dried. SA161 grown on 7H11 OADC plates at 37 °C for 3 weeks as the "*in vitro*" LAM culture control was also subjected to organic extractions directly as described omitting any homogenization or enzyme treatment steps.

Purification of Mlung-LAM

LAM isolated from *in vitro* grown bacilli and from the granulomas were subjected to hydrophobic interaction column chromatography using Octyl Sepharose 4 FAST FLOW chromatography [23]. The column was eluted with a buffer of 0.1 M ammonium acetate containing a stepwise gradient of 15%, 40% and 65% 1-propanol (pH 4.6), the three fractions were collected and dried under N_2. LAM eluted at 40% propanol fraction was used for subsequent analysis.

Cellulomonas endoarabinanase digestion followed by LC/MS Analyses

About 1 μg of Cul-LAM and MlungLAM LAM were mixed with *Cellulomonas gelida* endo-arabinanase respectively and incubated at 37°C overnight. An aliquot of samples was analyzed by SDS-PAGE followed by Periodic acid–Schiff (PAS)-silver staining to ensure complete digestion of LAMs. The purified lipoglycans was the mixture of LAM and LM. The digestion products containing both the mannan core, the released oligoarabinosides and LMs were separated using nanosep 3K omega (Pall Corporation) and centrifuging at 14,000 × g for 20 min at RT. The released oligoarabinosides in the flow through were analysed by LC/MS either in the native form or after reduction by using 1 mg/mL sodium borodeuteride and then permethylated using the NaOH/dimethyl sulfoxide slurry method as described [46].

The reduced and methylated samples were analyzed on an Agilent 6220 time-of-flight mass spectrometer interfaced to an Agilent 1200 high performance liquid chromatograph. Separation was performed in gradient mode with a Waters X-Bridge C18 HPLC 3.5 um

column (2.1 × 150 mm) at 40 °C. Mobile phase components were 0.1% formic acid in water (A) and 0.1 formic acid in acetonitrile (B). The flow rate was 0.32 mL/min. The proportion of acetonitrile was held at 10% for 5 min, then increased to 100% over 11 min, held at 100% for 4 min. The injection volume was 4 μL. MS data were acquired in mixed positive electrospray and atmospheric pressure chemical ionization mode (ESI/APCI) mode with a mass-to-charge ratio (*m/z*) range of 200 to 3200 at 1.3 Hz scan rate. Source settings were: source temperature 310 °C, vaporizer 200 °C, gas flow 10.0 L/min, nebulizer pressure 45 psi, Vcharge 2000 V, capillary 3000 V, fragmentor 40 V, and skimmer 60 V.°C. Internal instrument mass-scale calibration was performed by infusing Agilent ESI-L low concentration tuning mix during the acquisition run. Instrument controls and data processing were performed via the Agilent MassHunter B5.0 software package.

LC/MS-MS conditions for native arabinofuranosides

Structural elucidation was carried out via ultra-performance liquid chromatography (UPLC) separation on a Waters Acquity UPLC H-Class system inline with a Bruker MaXis Plus quadrupole time of flight (QTOF) mass spectrometer (MS). Separation was performed in gradient mode with a Waters Atlantis T3 3.0 um column (2.1 × 150 mm) at 40 °C. Mobile phase components were 10 mM ammonium acetate in water (A) and 10 mM ammonium acetate in acetonitrile (B). The flow rate was 0.3 mL/min. The proportion of acetonitrile was held at 0% for 1 minute, then increased from 0% to 95% in 9 min, held at 100% for 3 min. The post-time was 7 min and injection volume 4 μL. For full scan experiments, data were acquired in the negative electrospray ion (ESI) mode with a mass-to-charge ratio (*m/z*) range of 110–4000 at 1Hz scan rate. Source settings were: capillary voltage 3500V, end-plate offset 500V, nebulizer gas pressure 3 bar, drying gas flow 10 L/min, and drying temperature 300 °C. For MS/MS experiments the sources settings noted above were the same except from the 2 – 6 minutes time segment, the MS was in multiple reaction monitoring (MRM) scan mode with collision-induced dissociation (CID) energies of 40eV on target masses with *m/z* width of 10 Daltons. Internal instrument mass-scale calibration was performed in enhanced quadratic mode during chromatographic dead time by infusing Agilent ESI-L low concentration tuning mix. Instrument controls were performed via the Bruker HyStar v4.1 software package. Data were processed using Bruker Compass 2.0 Data Analysis 4.4 software.

U-LAM processing

Clinically positive TB patient's urine samples PB2 and PB4 were obtained from FIND and originated from Peru. These samples were anonymous. To process ~40 mL of each sample, (estimated by GC/MS to have 1.6 μg and 1.0 μg of LAM in PB2 and PB4 respectively), we subjected these to a 3.5 kDa centricon (4 × 1000 rpm, 30 min X 3) to remove small molecule impurities that could interfere with the enzyme-digested fragments (<3 KDa) and also reduce the volume to ~5 mL in the retentate. Samples after drying were reconstituted in 500 μL of sterile water, and the arabinanase (100 μL) was added and incubated at 37°C for 12 h. After enzyme inactivation at −80°C (2h) followed by a brief heating at 80°C, we subjected these to a second 3.5 KDa centricon (4 × 1000 rpm, 30 min X 3) and collected the digested fragments as Flow-through. The samples were lyophilized and PB2 was subjected to ESI-LC/MS directly and we subjected PB4 to reduction-permethylation sequence using sodium

borohydride followed by the treatment with methyl iodide in sodium hydroxide-DMSO for per-*O*-mehylation [46].

Supplementary Material

Refer to Web version on PubMed Central for supplementary material.

Acknowledgements

We acknowledge Funding from the National Institutes of Health (NIH) 1R21AI094338 to LS and RO1 AI1R01AI132680 to DC. We gratefully acknowledge Ms. Anita Amin for purifying and providing the *Cellulomonas gelida* endoarabinanase and the Central Instrument Facilities for LC/MS services. We would also like to thank the Foundation of Innovative Research (FIND) for provision of the bulk Peru urine samples.

References

1. WHO WHO Global Tuberculosis Report; Geneva, 10 17,2019, 2019.
2. WHO Global Tuberculosis Report ISBN 978 92 4 156539 4; WHO: Geneva, 2016; pp 1–214.
3. McNerney R; Maeurer M; Abubakar I; Marais B; McHugh TD; Ford N; Weyer K; Lawn S; Grobusch MP; Memish Z; Squire SB; Pantaleo G; Chakaya J; Casenghi M; Migliori GB; Mwaba P; Zijenah L; Hoelscher M; Cox H; Swaminathan S; Kim PS; Schito M; Harari A; Bates M; Schwank S; O'Grady J; Pletschette M; Ditui L; Atun R; Zumla A, Tuberculosis diagnostics and biomarkers: needs, challenges, recent advances, and opportunities. J Infect Dis 2012, 205 Suppl 2, S147–58. [PubMed: 22496353]
4. Chatterjee D; Bozic CM; McNeil M; Brennan PJ, Structural features of the arabinan component of the lipoarabinomannan of Mycobacterium tuberculosis. J Biol Chem 1991, 266 (15), 9652–9660. [PubMed: 1903393]
5. Chatterjee D; Hunter SW; McNeil M; Brennan PJ, Lipoarabinomannan. Multiglycosylated form of the mycobacterial mannosylphophatidylinositols. J. Biol. Chem. 1992, 267, 6228–6233. [PubMed: 1556131]
6. Chatterjee D; Lowell K; Rivoire B; McNeil M; Brennan PJ, Lipoarabinomannan of Mycobacterium tuberculosis. Capping with mannosyl residues in some strains. J. Biol. Chem. 1992, 267, 6234–6239. [PubMed: 1556132]
7. Murase M; Kano M; Tsukahara T; Takahashi A; Torigoe T; Kawaguchi S; Kimura S; Wada T; Uchihashi Y; Kondo T; Yamashita T; Sato N, Side population cells have the characteristics of cancer stem-like cells/cancer-initiating cells in bone sarcomas. Br J Cancer 2009, 101 (8), 1425–32. [PubMed: 19826427]
8. Rademacher C; Shoemaker GK; Kim HS; Zheng RB; Taha H; Liu C; Nacario RC; Schriemer DC; Klassen JS; Peters T; Lowary TL, Ligand specificity of CS-35, a monoclonal antibody that recognizes mycobacterial lipoarabinomannan: a model system for oligofuranoside-protein recognition. J Am Chem Soc 2007, 129 (34), 10489–502. [PubMed: 17672460]
9. Kaur D; Lowary TL; Vissa VD; Crick DC; Brennan PJ, Characterization of the epitope of anti-lipoarabinomannan antibodies as the terminal hexaarabinofuranosyl motif of mycobacterial arabinans. Microbiology 2002, 148 (Pt 10), 3049–57. [PubMed: 12368438]
10. Amin AG; De P; Spencer JS; Brennan PJ; Daum J; Andre BG; Joe M; Bai Y; Laurentius L; Porter MD; Honnen WJ; Choudhary A; Lowary TL; Pinter A; Chatterjee D, Detection of lipoarabinomannan in urine and serum of HIV-positive and HIV-negative TB suspects using an improved capture-enzyme linked immuno absorbent assay and gas chromatography/mass spectrometry. Tuberculosis (Edinb) 2018, 111, 178–187. [PubMed: 30029905]
11. Choudhary A; Patel D; Honnen W; Lai Z; Prattipati RS; Zheng RB; Hsueh YC; Gennaro ML; Lardizabal A; Restrepo BI; Garcia-Viveros M; Joe M; Bai Y; Shen K; Sahloul K; Spencer JS; Chatterjee D; Broger T; Lowary TL; Pinter A, Characterization of the Antigenic Heterogeneity of Lipoarabinomannan, the Major Surface Glycolipid of Mycobacterium tuberculosis, and

Complexity of Antibody Specificities toward this Antigen. J Immunol 2018, 200 (9), 3053–3066. [PubMed: 29610143]

12. Khoo KH; Douglas E; Azadi P; Inamine JM; Besra GS; Mikusová K; Brennan PJ; Chatterjee D, Truncated structural variants of lipoarabinomannan in ethambutol drug-resistant strains of Mycobacterium smegmatis - Inhibition of arabinan biosynthesis by ethambutol. J.Biol. Chem. 1996, 271, 28682–28690. [PubMed: 8910503]
13. Rivoire B; Ranchoff B; Chatterjee D; Gaylord H; Tsang A; Kolk AHJ; Aspinall GO; Brennan PJ, Generation of monoclonal antibodies to the specific sugar epitopes of Mycobacterium avium complex serovars. Infect.Immun. 1989, 57, 3147–3158. [PubMed: 2476400]
14. Singh KK; Dong Y; Belisle JT; Harder J; Arora VK; Laal S, Antigens of Mycobacterium tuberculosis recognized by antibodies during incipient, subclinical tuberculosis. Clin Diagn Lab Immunol 2005, 12 (2), 354–8. [PubMed: 15699433]
15. Roberts-Thomson PJ; Shepherd K, Molecular size heterogeneity of immunoglobulins in health and disease. Clin Exp Immunol 1990, 79 (3), 328–34. [PubMed: 2317941]
16. Harraldson B; Nystrom J; Deen WM, Properties of the glomerular barrier and mechanisms of proteinuris. Physiol Rev 2008, 2008 (88), 451–487.
17. Wood R; Lawn SD, Challenges facing lipoarabinomannan urine antigen tests for diagnosing HIV-associated tuberculosis. Expert Rev Mol Diagn 2012, 12 (6), 549–51. [PubMed: 22845473]
18. Chatterjee D; Khoo KH, Mycobacterial lipoarabinomannan: an extraordinary lipoheteroglycan with profound physiological effects. Glycobiology 1998, 8 (2), 113–20. [PubMed: 9451020]
19. Kaur D; Berg S; Dinadayala P; Gicquel B; Chatterjee D; McNeil MR; Vissa VD; Crick DC; Jackson M; Brennan PJ, Biosynthesis of mycobacterial lipoarabinomannan: Role of a branching mannosyltransferase. Proc Natl Acad Sci U S A 2006, 103 (37), 13664–13669. [PubMed: 16945913]
20. Appelmelk BJ; den Dunnen J; Driessen NN; Ummels R; Pak M; Nigou J; Larrouy-Maumus G; Gurcha SS; Movahedzadeh F; Geurtsen J; Brown EJ; Eysink Smeets MM; Besra GS; Willemsen PT; Lowary TL; van Kooyk Y; Maaskant JJ; Stoker NG; van der Ley P; Puzo G; Vandenbroucke-Grauls CM; Wieland CW; van der Poll T; Geijtenbeek TB; van der Sar AM; Bitter W, The mannose cap of mycobacterial lipoarabinomannan does not dominate the Mycobacterium-host interaction. Cell Microbiol 2008, 10 (4), 930–44. [PubMed: 18070119]
21. Sigal GB; Pinter A; Lowary TL; Kawasaki M; Li A; Mathew A; Tsionsky M; Zheng RB; Plisova T; Shen K; Katsuragi K; Choudhary A; Honnen WJ; Nahid P; Denkinger CM; Broger T, A Novel Sensitive Immunoassay Targeting the 5-Methylthio-d-Xylofuranose-Lipoarabinomannan Epitope Meets the WHO's Performance Target for Tuberculosis Diagnosis. J Clin Microbiol 2018, 56 (12).
22. Angala SK; McNeil MR; Shi L; Joe M; Pham H; Zuberogoitia S; Nigou J; Boot CM; Lowary TL; Gilleron M; Jackson M, Biosynthesis of the Methylthioxylose Capping Motif of Lipoarabinomannan in Mycobacterium tuberculosis. ACS chemical biology 2017, 12 (3), 682–691. [PubMed: 28075556]
23. Treumann A; Xidong F; McDonnell L; Derrick PJ; Ashcroft AE; Chatterjee D; Homans SW, 5-Methylthiopentose: a new substituent on lipoarabinomannan in Mycobacterium tuberculosis. J. Mol. Biol. 2002, 316 (1), 89–100. [PubMed: 11829505]
24. Turner J; Torrelles JB, Mannose-capped lipoarabinomannan in Mycobacterium tuberculosis pathogenesis. Pathog Dis 2018, 76 (4).
25. Shi L; Ryan GJ; Bhamidi S; Troudt J; Amin A; Izzo A; Lenaerts AJ; McNeil MR; Belisle JT; Crick DC; Chatterjee D, Isolation and purification of Mycobacterium tuberculosis from H37Rv infected guinea pig lungs. Tuberculosis 2014, 94 (5), 525–530. [PubMed: 25037320]
26. Shang S; Harton M; Tamayo MH; Shanley C; Palanisamy GS; Caraway M; Chan ED; Basaraba RJ; Orme IM; Ordway DJ, Increased Foxp3 expression in guinea pigs infected with W-Beijing strains of M. tuberculosis. Tuberculosis 2011, 91 (5), 378–85. [PubMed: 21737349]
27. Kramnik I; Dietrich WF; Demant P; Bloom BR, Genetic control of resistance to experimental infection with virulent Mycobacterium tuberculosis. Proceedings of the National Academy of Sciences of the United States of America 2000, 97 (15), 8560–5. [PubMed: 10890913]

28. De P; Amin AG; Valli E; Perkins MD; McNeil M; Chatterjee D, Estimation of D-Arabinose by Gas Chromatography/Mass Spectrometry as Surrogate for Mycobacterial Lipoarabinomannan in Human Urine. PLoS One 2015, 10 (12), e0144088. [PubMed: 26633829]
29. Gaylord H; Brennan PJ; Young DB; Buchanan TM, Most Mycobacterium leprae carbohydrate-reactive monoclonal antibodies are directed to lipoarabinomannan. Infect.Immun. 1987, 55, 2860–2863. [PubMed: 3312018]
30. McNeil MR; Robuck KG; Harter M; Brennan PJ, Enzymatic evidence for the presence of a critical terminal hexa-arabinoside in the cell walls of Mycobacterium tuberculosis. Glycobiology 1994, 4 (2), 165–73. [PubMed: 8054716]
31. Chatterjee D; Khoo K-H; McNeil MR; Dell A; Morris HR; Brennan PJ, Structural definition of the non-reducing termini of mannose-capped LAM from Mycobacterium tuberculosis through selective enzymatic degradation and fast atom bombardment-mass spectrometry. Glycobiology 1993, 3, 497–506. [PubMed: 8286863]
32. De P; McNeil M; Xia M; Boot CM; Hesser DC; Denef K; Rithner C; Sours T; Dobos KM; Hoft D; Chatterjee D, Structural determinants in a glucose-containing lipopolysaccharide from Mycobacterium tuberculosis critical for inducing a subset of protective T cells. J Biol Chem 2018, 293 (25), 9706–9717. [PubMed: 29716995]
33. Harvey DJ, Fragmentation of negative ions from carbohydrates: Part 2. Fragmentation of high-mannose N-linked glycans. jJ of Amer. Soc. Mass Spectrom. 2005, 16, 631–646.
34. Demarque DP; Crotti AEM; Vessecchi R; Lopesa JLC; Lopes NP, Fragmentation reactions using electrospray ionization mass spectrometry: an important tool for the structural elucidation and characterization of synthetic and natural products. Natural Product Reports 2016, 33 (3), 432–455. [PubMed: 26673733]
35. Hunter SW; Gaylord H; Brennan PJ, Structure and antigenicity of the phosphorylated lipopolysaccharide antigens from the leprosy and tubercle bacilli. J. Biol. Chem. 1986, 261, 12345–12351. [PubMed: 3091602]
36. Bhamidi S; Scherman MS; Rithner CD; Prenni JE; Chatterjee D; Khoo KH; McNeil MR, The Identification and Location of Succinyl Residues and the Characterization of the Interior Arabinan Region Allow for a Model of the Complete Primary Structure of Mycobacterium tuberculosis Mycolyl Arabinogalactan. J Biol Chem 2008, 283 (19), 12992–3000. [PubMed: 18303028]
37. Palcekova Z; Angala SK; Belardinelli JM; Eskandarian HA; Joe M; Brunton R; Rithner C; Jones V; Nigou J; Lowary TL; Gilleron M; McNeil M; Jackson M, Disruption of the SucT acyltransferase in Mycobacterium smegmatis abrogates succinylation of cell envelope polysaccharides. J Biol Chem 2019, 294 (26), 10325–10335. [PubMed: 31110045]
38. Turnbull WB; Shimizu KH; Chatterjee D; Homans SW; Treumann A, Identification of the 5-methylthiopentosyl substituent in Mycobacterium tuberculosis lipoarabinomannan. Angew. Chem. Int Ed Engl 2004, 43 (30), 3918–22. [PubMed: 15274213]
39. Anthony LSD; Chatterjee D; Brennan PJ; Nano FE, Lipoarabinomannan from Mycobacterium tuberculosis modulates the generation of reactive nitrogen intermediates by gamma interferon-activated macrophages. FEMS Immunol.Med.Microbiol. 1994, 8, 299–306. [PubMed: 8061654]
40. Juffermans NP; Verbon A; Belisle JT; Hill PJ; Speelman P; van DS; van Der PT, Mycobacterial lipoarabinomannan induces an inflammatory response in the mouse lung. A role for interleukin-1 Am J Respir Crit Care Med 2000, 162 (2 Pt 1), 486–9. [PubMed: 10934075]
41. Strohmeier GR; Fenton MJ, Roles of lipoarabinomannan in the pathogenesis of tuberculosis. Microbes Infect 1999, 1 (9), 709–17. [PubMed: 10611748]
42. Torrelles JB; Knaup R; Kolareth A; Slepushkina T; Kaufman TM; Kang PB; Hill P; Brennan PJ; Chatterjee D; Belisle JT; Musser JM; Schlesinger LS, Identification of mycobacterium tuberculosis clinical isolates with altered phagocytosis by human macrophages due to a truncated lipoarabinomannan. J Biol Chem 2008, 283 (46), 31417–31428. [PubMed: 18784076]
43. Granoff DM; Donnelly JJ, A Modified ELISA for Measurement of High-Avidity IgG Antibodies to Meningococcal Serogroup C Polysaccharide that Correlate with Bactericidal Titers. Methods Mol Med 2001, 66, 305–15. [PubMed: 21336763]

44. Murase T; Zheng RB; Joe M; Bai Y; Marcus SL; Lowary TL; Ng KK, Structural insights into antibody recognition of mycobacterial polysaccharides. J Mol Biol 2009, 392 (2), 381–92. [PubMed: 19577573]

45. Ordway DJ; Shang S; Henao-Tamayo M; Obregon-Henao A; Nold L; Caraway M; Shanley CA; Basaraba RJ; Duncan CG; Orme IM, Mycobacterium bovis BCG-Mediated Protection against W-Beijing Strains of Mycobacterium tuberculosis Is Diminished Concomitant with the Emergence of Regulatory T Cells. Clinical and vaccine immunology : CVI 2011, 18 (9), 1527–35. [PubMed: 21795460]

46. Ciucanu I; Kerek F, A simple and rapid method for the permethylation of carbohydrates. Carbohydr. Res 1984, 131, 209–217.

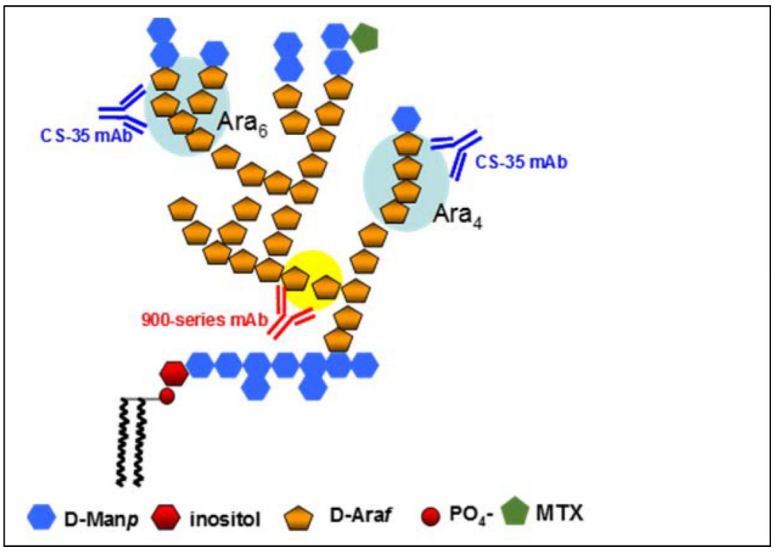

Fig. 1. Schematic representation
of the structure of *Mtb* LAM and binding epitopes of two major CSU anti-LAM mAbs.

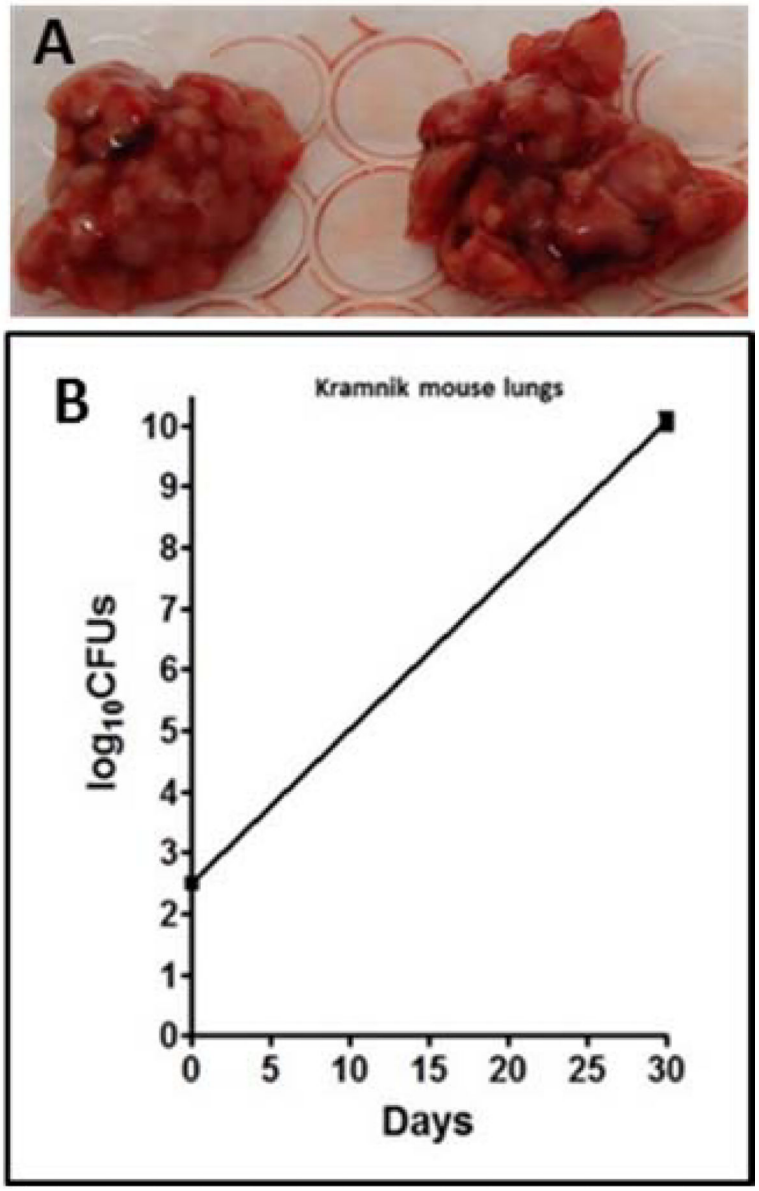

Fig. 2: Necrotic lungs after infection and CFU counts.

W. Beijing SA161 infected Kramnik mouse lungs (A); CFU counts result (B) on SA161 infected Kramnik mouse lung tissues.

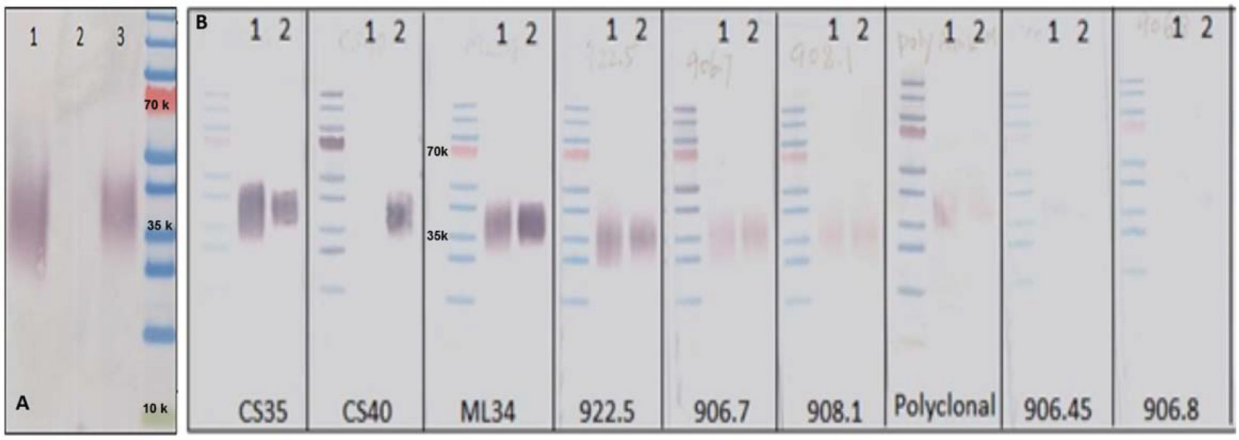

Fig. 3A: Detection of *M. tb* W. Beijing SA 161 LAM preparations
using immunoblotting with pooled mAbs. Lane 1, Cul- LAM; Lane 2, uninfected Lung control; Lane 3, Mlung-LAM **3B**: Detection of Mlung-LAM using immunoblotting with individual mAbs available in CSU. Lane 1: Cul-LAM; 2: Mlung-LAM. 50 ng of LAM was applied to each of the lanes based on GC/MS quantification of D-Arabinose (Supplementary Fig. S3).

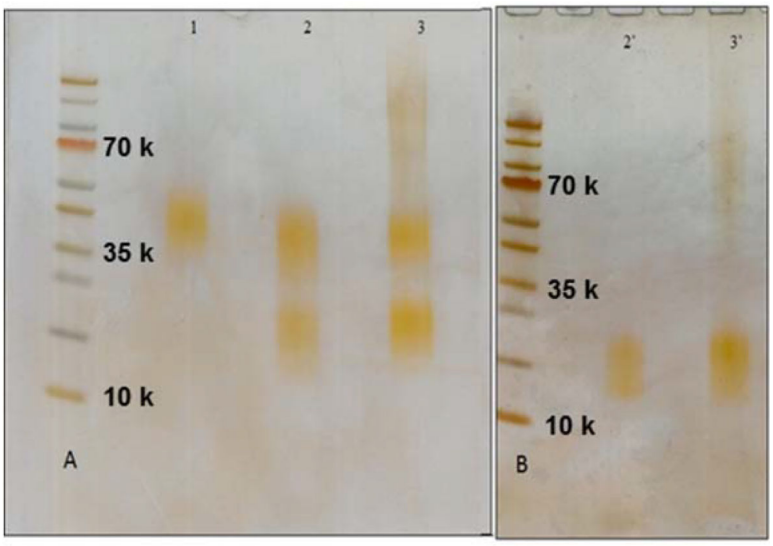

Fig. 4. Detection of purified LAM samples by SDS-PAGE followed by PAS staining.

A: 1, CDC1551 LAM (control); 2, SA 161 in vitro (LAM+LM); 3, SA 161 infected Mlung-LAM. B: 2', SA 161 Cul-LAM core after *Cellulomonas gelida* endoarabinanase digestion; 3', SA 161 Mlung-LAM core after endoarabinanase digestion.

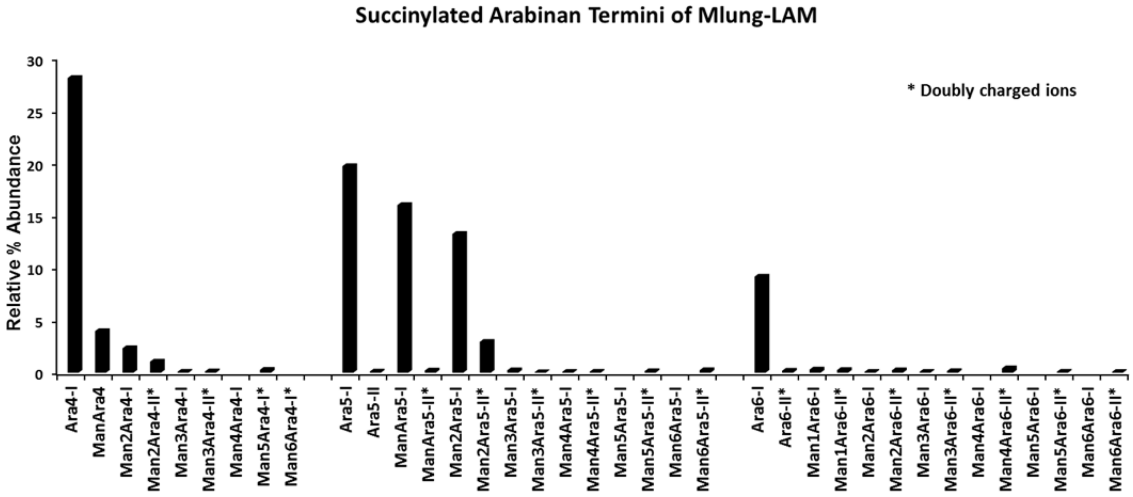

Fig. 5: Succinylated arabinan termini.

Relative % abundance (intensities of each ion were overall normalized) of succinylated arabinan termini, released after endoarabinanase digestion of Mlung-LAM. All asterix marked termini were found as doubly charged species except Ara_5-II which has a different retention time than Ara_5-I.

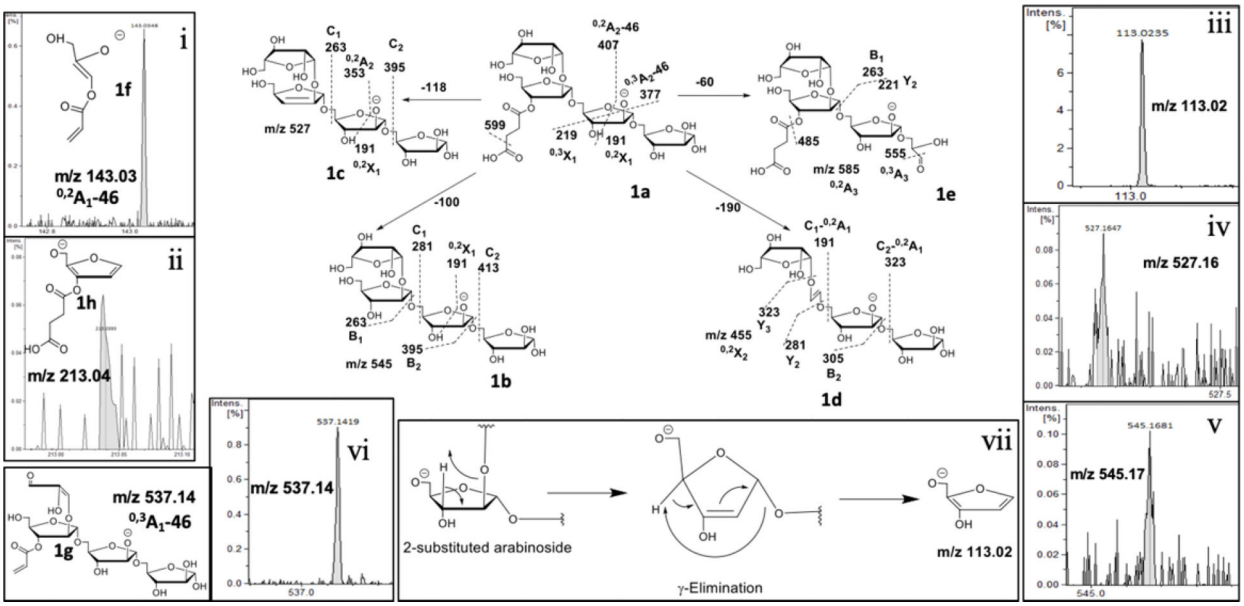

Fig 6. MS^2 fragmentation of succinylated Ara_4

(*m/z* 645 $(M-H)^{1-}$; **1a**) and the location of the succinyl substitution. Different pathways of fragmentation have been described with representative ions 1b-e.. i) A-type ion at m/z 143 corresponds to the structure **1f**. It shows the location of the succinyl residue (after α-cleavage) at the non-reducing side of Ara*f* unit. Only two possibilities identified; one, terminal β-linked Ara*f*; two, 2-glycosylated penultimate Ara*f*. ii) The ion at m/z 213, corresponding to **1g**, shows that the succinyl residue is at the 3-position of the 2-glycosylated Ara*f*. iii) The ion at *m/z* 113 is characteristic of furan ring formation. iv & v) The ions at *m/z* 527 and 545 supports the loss of a succinyl residue attached to a secondary –OH group. vi) The ion *m/z* 537 and its assigned structure signifying terminal Ara*f* has unsubstituted 3-and 5-OH groups. vii) Plausible mechanism of formation of *m/z* 113 through a γ-elimination, common in CID-MS^2.

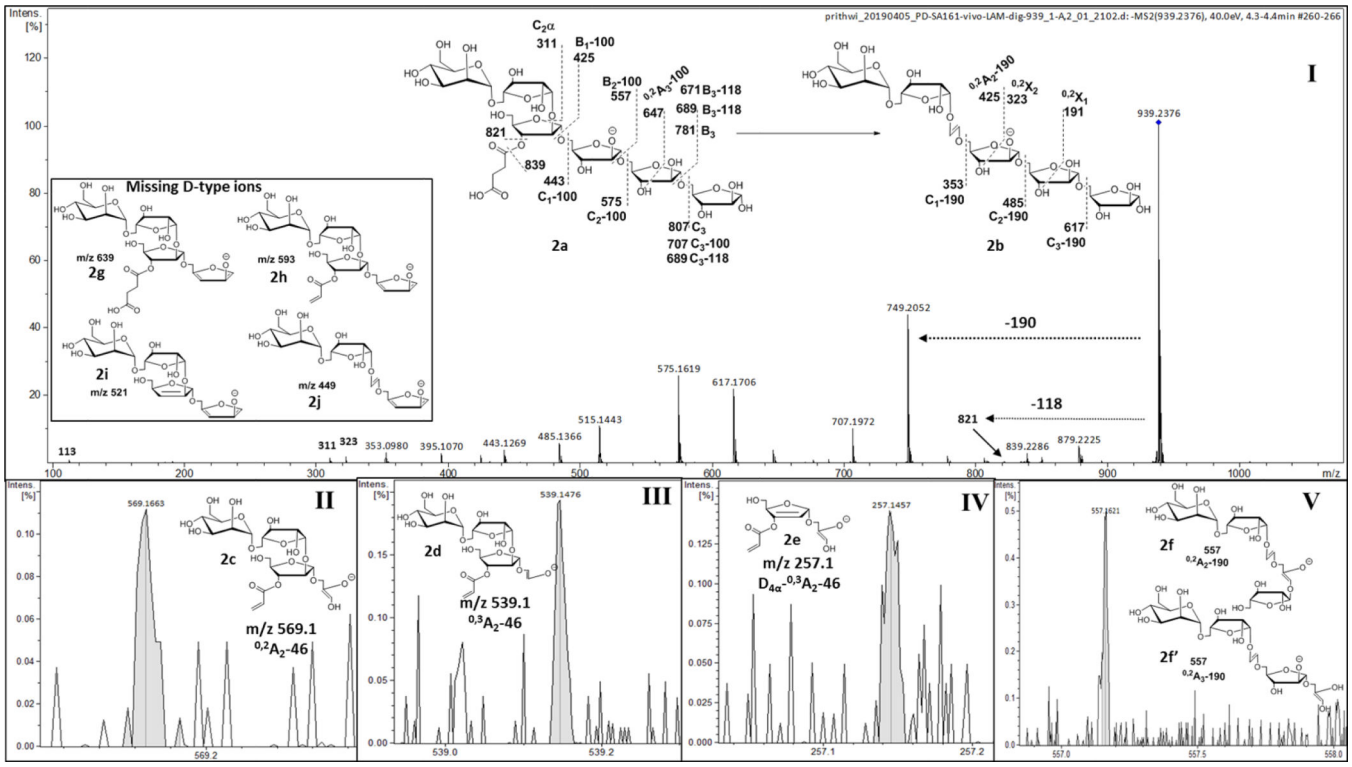

Fig 7: MS^2 fragmentation of succinylated Man$_1$Ara$_5$

(*m/z* 939 (M-H)$^{1-}$; **2a**) identifying dominant linear arrangement of Ara$_5$ termini. I) MS^2 profile of 2a and representative fragmentations. II, III & IV) Fragment ions confirming the location of the succinyl residue at the 3-position of 2-glycosylated Ara*f*. V) The ion at *m/z* 557 corresponding to structures **2f** and **2f'** represents the possibility of Ara5-skeleton being linear or branched. Inset) Missing ions (**2g-j**) would have confirmed a branched structure.

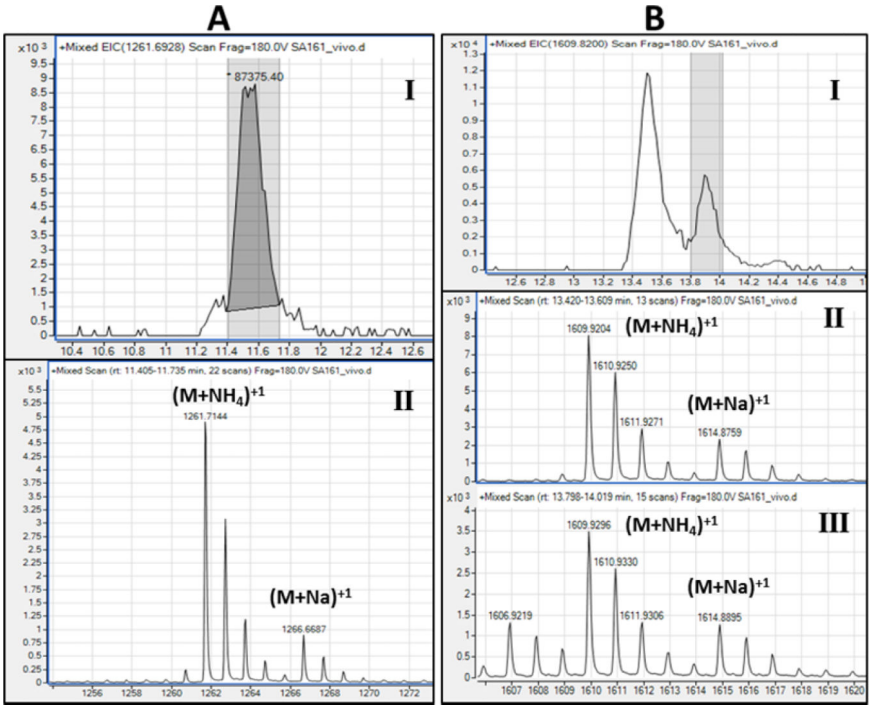

Fig. 8:

A) Presence of MTXMan$_1$Ara$_5$ (*m/z* 1261.7; M + NH_4^+) as detected (panel I) chromatogram; Panel II) Extracted ion) by ESI-LC/MS (positive ion) using borodeuteride-reduction and methyl iodide-permethylation of arabinan fragments. **B**) The EIC of *m/z* 1609.9 $(M+NH_4)^{+1}$ from Mlung-LAM corresponds to permethylated Man$_2$Ara$_7$ as well as permethylated Man$_4$Ara$_4$Lactate two peaks are present (panel I) in EIC shows the same ion from Left (II) and Right (III) peak showing the possible presence of both arabinan termini.

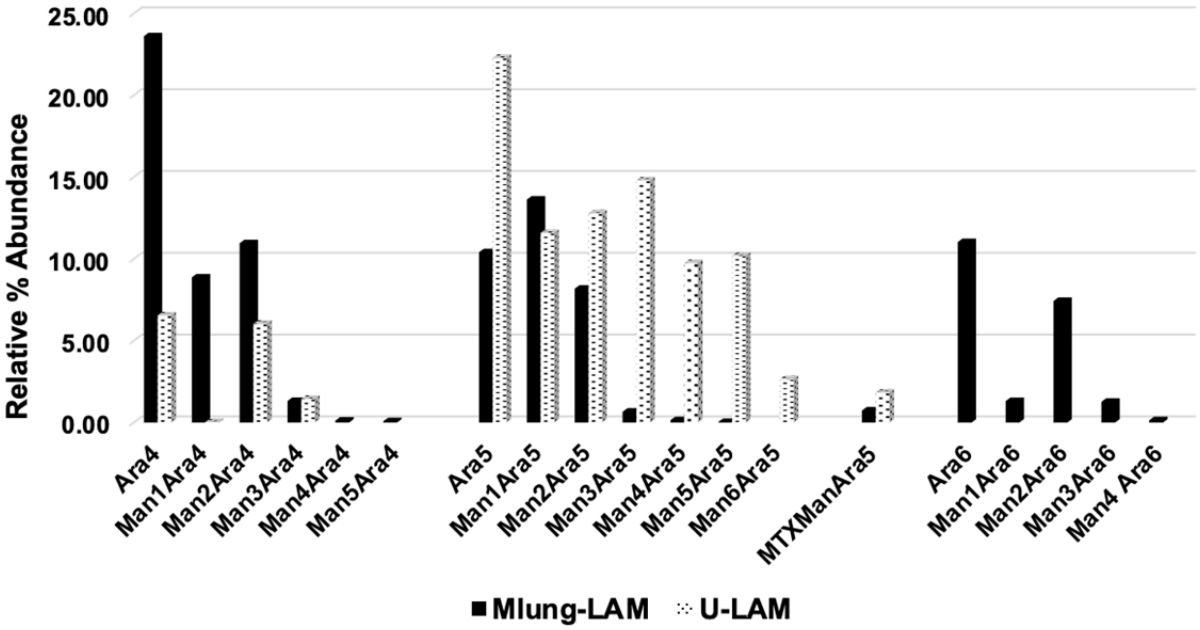

Fig. 9: Non reducing arabinan termini of Mlung-LAM and U-LAM.

Comparative bar plot of Relative % abundance (intensities of each ion were overall normalized) of arabinan termini released after endoarabinanase digestion of Mlung-LAM and u-LAM followed by reduction, permethylation and LC/MS. Decrease in Ara_4 and Ara_6 termini (including mannose capped ones) and increase in Ara_5 termini are evident in U-LAM in comparison to Mlung-LAM. All the acyl functions will be lost during methylation.